WIS-81/57 Dec-PH

Polarization of Recoil Deuteron in ed Elastic Scattering at Medium Energies

R. S. BHALERAO

Department of Nuclear Physics

Weizmann Institute of Science

Rehovot, Israel

Abstract

Vector and tensor polarizations of the recoil deuteron in ed elastic scattering are calculated for $\theta=0^{o}$-180^{o} and $q^{2}\leq 8(\mathrm{GeV/c})^{2}$. A longitudinally polarized electron beam is assumed to scatter off an unpolarized deuteron target. Calculations are made in the relativistic impulse approximation using a recently described approach based on the Bethe-Salpeter equation. Results are different, at high q^{2} even qualitatively so, from those of a non-relativistic calculation, and a relativistic calculation which takes the spectator nucleon on-mass-shell. In the light of these results a recent suggestion that the polarization measurements would throw new light on the off-shell behavior and tensor force strength of the NN interaction are reexamined. Results are also presented for the three deuteron form factors G_{C}, G_{Q}, and G_{M}, and the often-needed related quantities S_{S}, S_{Q}, and S_{M}. The latter results may have an important implication in high-momentum transfer reactions involving deuteron.

1. Introduction

Measurements of polarization in ed elastic scattering are necessary if the deuteron charge-, quadrupole-, and magnetic dipole form factors, $G_C(q^2)$, $G_Q(q^2)$, and $G_M(q^2)$ are to be determined uniquely. This is because measuring the ed elastic differential cross section alone provides us with only two linear combinations of G_C^2, G_Q^2, and G_M^2. For, the differential cross section of ed elastic scattering is given by[1)]

$$\frac{d\sigma}{d\Omega} = \left(\frac{d\sigma}{d\Omega}\right)_{\text{Mott}} [A(q^2)+B(q^2)\tan^2(\tfrac{1}{2}\theta)], \tag{1}$$

where

$$A(q^2)=G_C^2+\frac{8}{9}\eta^2 G_Q^2+\frac{2}{3}\eta G_M^2,$$

$$B(q^2)=\frac{4}{3}\eta(1+\eta)G_M^2,$$

$$\eta=\frac{q^2}{4M_D^2}, \tag{2}$$

$\left(\frac{d\sigma}{d\Omega}\right)_{\text{Mott}}$ is the Mott cross section, M_D is the deuteron mass, q^2 the four-momentum transfer squared, and θ the laboratory scattering angle of the electron. Measurements of the cross section can thus determine only the structure functions A and B; and polarization measurements are needed if G_C is to be separated from G_Q.

Experimental data for the structure functions $A(q^2)$ and $B(q^2)$ are available upto $q^2 \approx 8(\text{GeV/c})^2$ and $q^2 = 1(\text{GeV/c})^2$ respectively [2,3]. No data are presently available for the polarization transfer in ed elastic scattering. Before one calculates the polarization components it is obviously important that the theory to be tested should reproduce the experimental values of $A(q^2)$ and $B(q^2)$. Calculation of these structure functions is often made in the impulse approximation assuming the scattering to proceed through the one-photon-exchange triangle diagram[1]. Non-relativistic calculations of $A(q^2)$ tend to underestimate the data for $q^2 \gtrsim 1.5(\text{GeV/c})^2$, the disagreement becoming worse as q^2 increases. Extensive relativistic calculations by Arnold, Carlson, and Gross [4] with two- and four-component deuteron wave functions, different models for the nucleon-nucleon (NN) interaction, and various sets of electromagnetic form factors of nucleon failed to bridge the gap. In fact the relativistic results of ref.[4] were smaller than the nonrelativistic ones, thereby worsening the disagreement with the data. Exchange current effects have been proposed as a possible cure for this discrepancy [5]. As regards the magnetic structure function $B(q^2)$, relatively few data are available, and they are in fair agreement with nonrelativistic calculations [3].

We recently presented relativistic calculations of $A(q^2)$ and $B(q^2)$ which were in satisfactory agreement with all the available data, without having to include the exchange-current contribution [6]. Here we describe the salient features of this approach. The details can be found in refs. [6,7]. These calculations were based on the relativistic impulse approximation

making use of the triangle diagram. It was shown that a very important relativistic kinematical effect is associated with the Lorentz transformation from the Breit frame in which the deuteron is moving to the deuteron rest frame where the deuteron wave function is computed [6]. In order to perform the Lorentz transformation one needs to know the energy and momentum of the target nucleon undergoing the transformation. This in turn requires some assumption regarding whether the nucleon is on-mass-shell or not. Different assumptions lead to different values of the pn relative momentum in the deuteron rest frame. Considering the sensitivity of the deuteron momentum space wave functions the above effect can lead to significantly different values for the structure functions. Now as in ref. [4] if the spectator nucleon in the triangle diagram is taken on-mass-shell, then in the region of the momentum space which is expected to contribute most to the form factors, the pn relative momentum in the deuteron rest frame tends to be larger than the nonrelativistic value[6]. This in general tends to reduce the relativistic form factor compared to the nonrelativistic one. This we think is the reason why the relativistic calculations of ref.[4] gave results for $A(q^2)$ which were smaller than the corresponding non-relativistic results.

A new treatment of this problem in the framework of the Bethe-Salpeter equation with the ladder approximation was described in refs.[6,7]. In ref.[7] a 3-dimensional reduction of the Bethe-Salpeter equation was carried out without neglecting the meson production singularities of the dpn vertex function. Negative energy poles of the nucleon propagators being far away from the physical region were neglected. One of the

final results of this work was that in the expression for the deuteron form factor as an overlap of deuteron momentum space wave functions, each wave function should be replaced by the average of two wave functions: One of these is evaluated at pn relative momentum in the deuteron rest frame obtained by keeping one of the two nucleons on-mass-shell; the other corresponds to the other nucleon being on-mass-shell. Limitations of this approach are described in refs. [6,7]. As mentioned above calculations based on this approach gave very good agreement with all the available data for $A(q^2)$ and $B(q^2)$ [6]. In the present work we study the polarization transfer in ed elastic scattering in the framework of the above approach. Theory is described in sect. 2, which is followed by a description of our results in sect. 3, and a discussion in sect. 4.

2. Theory.

Deuteron charge-, quadrupole-, and magnetic form factors $G_C(q^2)$, $G_Q(q^2)$, and $G_M(q^2)$ are given by [1]

$$G_C(q^2)=C_E^o(q^2)G_E^S(q^2),$$

$$G_Q(q^2)=C_E^2(q^2)G_E^S(q^2),$$

and

$$G_M(q^2)=C_E^1(q^2)G_E^S(q^2)+C_M^1(q^2)G_M^S(q^2). \qquad (3)$$

Here $G_E^S=G_E^p+G_E^n$ and $G_M^S=G_M^p+G_M^n$ are nucleon isoscalar electromagnetic form factors, and the momentum space expressions for $C_{E,M}^i$ can be shown to be

$$C_E^o=I_1+I_2,$$

$$C_E^1=3M_D(I_2+I_4)/(4M_N),$$

$$C_E^2=6\sqrt{2}M_D^2(I_3-\frac{I_4}{2\sqrt{2}})/q^2,$$

and

$$C_M^1=M_D(I_1-\frac{I_2-I_4}{2}+\frac{I_3}{\sqrt{2}})/M_N. \qquad (4)$$

M_N is the nucleon mass, and

$$I_1 \equiv \int U(|\underset{\sim}{Q}-\tfrac{1}{2}\underset{\sim}{q}|)U(|\underset{\sim}{Q}+\tfrac{1}{2}\underset{\sim}{q}|)\,\frac{d\underset{\sim}{Q}}{4\pi},$$

$$I_2 \equiv \int W(|\underset{\sim}{Q}-\tfrac{1}{2}\underset{\sim}{q}|)W(|\underset{\sim}{Q}+\tfrac{1}{2}\underset{\sim}{q}|)P_2(Z_{+-})\,\frac{d\underset{\sim}{Q}}{4\pi},$$

$$I_3 \equiv \tfrac{1}{2}\int [U(|\underset{\sim}{Q}-\tfrac{1}{2}\underset{\sim}{q}|)W(|\underset{\sim}{Q}+\tfrac{1}{2}\underset{\sim}{q}|)P_2(Z_+)+U(|\underset{\sim}{Q}+\tfrac{1}{2}\underset{\sim}{q}|)W(|\underset{\sim}{Q}-\tfrac{1}{2}\underset{\sim}{q}|)P_2(Z_-)]\,\frac{d\underset{\sim}{Q}}{4\pi},$$

and

$$I_4 \equiv \tfrac{1}{2}\int W(|\underset{\sim}{Q}-\tfrac{1}{2}\underset{\sim}{q}|)W(|\underset{\sim}{Q}+\tfrac{1}{2}\underset{\sim}{q}|)(1-3Z_+Z_-Z_{+-})\,\frac{d\underset{\sim}{Q}}{4\pi}. \qquad (5)$$

U and W are S- and D-state wave functions of deuteron,

$Z_{\pm} \equiv \cos(\widehat{\underset{\sim}{Q}\pm\tfrac{1}{2}\underset{\sim}{q},\underset{\sim}{q}})$, and $Z_{+-} \equiv \cos(\widehat{\underset{\sim}{Q}+\tfrac{1}{2}\underset{\sim}{q},\underset{\sim}{Q}-\tfrac{1}{2}\underset{\sim}{q}})$. The quantities S_S, S_Q and S_M are related to C_E^o, C_E^2 and C_M^1 as follows

$$C_E^o(q^2)=S_S(\tfrac{q}{2}),$$

$$C_E^2(q^2)=\sqrt{18}\,M_D^2\,S_Q(\tfrac{q}{2})/q^2,$$

and

$$C_M^1(q^2)=M_D\,S_M(\tfrac{q}{2})/M_N. \qquad (6)$$

The above form factors are used in the calculation of vector and tensor polarizations of the recoil deuteron in ed elastic scattering. In this calculation we assume a longitudinally polarized electron beam to be scattered off an unpolarized deuteron target. Polarization transfer due to transversely polarized electrons is expected to be much smaller, of the order of m_e/E_e^{lab} [8], and hence is not calculated.

The non-vanishing vector and tensor polarizations are given by [9,10,11]

$$I_o p_x = -\frac{4}{3}[\eta(1+\eta)]^{\frac{1}{2}} G_M (G_C + \frac{1}{3}\eta G_Q) \tan(\tfrac{1}{2}\theta),$$

$$I_o p_z = \frac{2}{3}\eta\{(1+\eta)[1+\eta \sin^2(\tfrac{1}{2}\theta)]\}^{\frac{1}{2}} G_M^2 \quad \tan(\tfrac{1}{2}\theta)\sec(\tfrac{1}{2}\theta),$$

$$-I_o p_{zz} = \frac{8}{3}\eta G_C G_Q + \frac{8}{9}\eta^2 G_Q^2 + \frac{1}{3}\eta[1+2(1+\eta)\tan^2(\tfrac{1}{2}\theta)] G_M^2 ,$$

$$I_o (p_{xx} - p_{yy}) = -\eta G_M^2 ,$$

$$I_o p_{xz} = -2\eta[\eta+\eta^2 \sin^2(\tfrac{1}{2}\theta)]^{\frac{1}{2}} G_M G_Q \sec(\tfrac{1}{2}\theta) , \qquad (7)$$

where $I_o = A + B\tan^2(\tfrac{1}{2}\theta)$. We will also need the spherical tensor polarizations which are related to the Cartesian tensors given above as follows:

$$T_{20} = p_{zz}/\sqrt{2} ,$$

$$T_{21} = -p_{xz}/\sqrt{3},$$

and

$$T_{22} = (p_{xx} - p_{yy})/(2\sqrt{3}). \qquad (8)$$

It should be noted that the tensor polarizations p_{zz}, $(p_{xx}-p_{yy})$, and p_{xz} calculated in the one-photon-exchange approximation are independent of the polarization of the incident electron, and hence can be measured with even an unpolarized electron beam[11].

3. Results.

Our results for G_C, G_Q, and G_M are presented in figs. 1 a,b,c, and those for S_S, S_Q, and S_M in figs. 2 a,b,c. The recoil deuteron polarizations as a function of θ at many fixed values of $q^2 \leq 6 (GeV/c)^2$ are given in figs. 3 a,b,c, while those as a function of q^2 for a fixed θ ($\approx 40^o$) are given in figs. 4 a-f. The angle $\theta = 40^o$ was chosen only to facilitate a comparison with the results of Arnold et al.[11]. Fig. 5 where we plot $T_{20}(\theta \approx 0^o)$ and $T_{21}(\theta \approx 90^o)$ as a function of q fm^{-1} is meant only for a quick comparison with the results of Haftel et al.[10]. In figs. 1-5 dashed curves represent nonrelativistic calculations, and dotted curves represent our relativistic calculations performed with the spectator N in the triangle diagram on-mass-shell[6]. The solid curves are our predictions based on a calculation that starts with the relativistic Bethe-Salpeter equation. This approach is outlined above in sect. 1. In all our calculations we used the empirical dipole nucleon form factors with scaling, and G_E^n was set equal to zero. The Reid soft-core NN interaction[12] was used to calculate the S- and D-state wave functions of deuteron needed in the calculation of G_C, G_Q and G_M.

4. Discussion

As mentioned above the dotted curves in figs. 1 - 5 represent our relativistic calculations performed with the spectator N on-mass-shell. In ref. [6] these calculations gave results for $A(q^2)$ and $B(q^2)$, which were almost identical to the corresponding results of Arnold et al. [4]. Calculations in ref. [4] were also performed with the spectator N on-mass-shell, but they included additional effects, e.g. the pair-current effect, which are absent in our work. The dotted curves in fig. 4 are also similar to the relativistic results presented by Arnold et al. in ref. [11], the differences may be attributed mostly to their use of different deuteron wave functions and/or the so-called 'best-fit' nucleon form factors.

The solid curves in figs. 1 - 5 which are our predictions for these quantities are evidently quite different from the dashed and dotted curves. Consider first figs. 1 and 2. In the low momentum region ($q^2 < 3$ $(GeV/c)^2$ say) the minima in the solid curves are seen to be shifted to the right of the minima in other curves. In the high momentum region, on the other hand, the minima in the dashed and dotted curves are found to be absent in the solid curves.[7] Moreover magnitudes of the various curves are also different. The quantities S_S, S_Q, and S_M are often needed in reactions and scattering involving deuteron. For example, the cross section for pd backward scattering in the single scattering approximation is directly proportional to $(S_S^2+S_Q^2)$ [15]. It is expected that the results for S_S, S_Q, and S_M presented in fig. 2 would have an important implication in this and other high momentum transfer reactions involving deuteron. Calculations of the tensor analyzing power in pd backward scattering at GeV energies are in progress and will be reported later.

The aforementioned broad features of the deuteron form factors can be seen to be reflected in the polarizations in figs. 4 a-f. For $q^2 \lesssim 1.5$ (GeV/c)^2 the solid and dotted curves in fig. 4 tend to lie on opposite sides of the dashed curve. At higher q^2 the solid curves in fig. 4 are even qualitatively different from the dashed and dotted curves. As in the case of the form factors (fig. 1), the solid curves in fig. 4 do not exhibit minima or maxima in the region $q^2 > 3$(GeV/c)^2, while the dashed and dotted curves do. Particularly interesting is the ratio p_x/p_{xz} shown in fig. 4f. Experiments are being planned to measure p_x/p_{xz} near $q^2 = 1$ (GeV/c)^2, especially to determine the point at which it changes its sign[14]. According to our calculations at $\theta = 40^\circ$ the solid curve in fig. 4f, crosses the q^2 axis at $q^2 \sim 1.145$ (GeV/c)^2, while the dashed and dotted curves do so at $q^2 \sim 1.040$ (GeV/c)^2 and $q^2 \sim 0.925$ (GeV/c)^2 respectively. Almost the same numbers are obtained if $\theta = 90^\circ$. It is important to note that the solid curve crosses the q^2 axis at a higher momentum while the dotted curve crosses it at a lower momentum when compared with the (nonrelativistic) dashed curve. All the relativistic curves in ref.[11] also cross the q^2-axis at a lower momentum compared to the nonrelativistic curve.

In the high momentum region the discontinuities in the dashed and dotted curves in fig. 4f are the consequence of the minima in $|G_Q|$ present only in the dashed and dotted curves of fig. 1b. Of course the use of nonrelativistic wave functions of deuteron for such high momentum transfers is questionable, and it is hoped that errors introduced due to our use of nonrelativistic wave functions are not large. This point is discussed in refs.[6,7]. Here we only point out that the results obtained by Arnold et al.

for $A(q^2 \lesssim 8(\mathrm{GeV/c})^2)$, $B(q^2 \lesssim 8(\mathrm{GeV/c})^2)$ and the polarization transfer $(q^2 \lesssim 2(\mathrm{GeV/c})^2)$ with 4-component relativistic wave functions of deuteron are not very much different from those obtained with 2-component nonrelativistic wave functions. [4,11].

The sensitivity of the deuteron structure functions to the choice of the N electromagnetic form factors has been studied by Arnold et al. [4]. They used three different sets of nucleon form factors other than the dipole form, and found that the results for $q^2 < 6(\mathrm{GeV/c})^2$ differed very little from each other with the exception of those based on the Iachello, Jackson, and Lande (IJL) nucleon form factors [15].

(This is because of the unreasonable [4] behavior of G_E^n in the IJL form factors). However, a similar effect in the calculation of the polarization components of deuteron is unclear. In this context it is interesting to note that the polarization T_{20} (eq. 8) is sometimes calculated at an extrapolated θ so as to kill the G_M-dependence [9]. The extrapolated T_{20} is independent of the nucleon form factors, and depends only on the ratio of G_C and G_Q. Our results for this quantity were given in ref. [6]. Similarly the ratio p_x/p_{xz} is also independent of the nucleon form factors [11].

In this paper we used the Reid soft-core NN interaction [12] to calculate the polarization components of the recoil deuteron. In ref. [6] we studied the sensitivity of the deuteron structure functions to the NN interaction by using the Reid soft-core, Paris [16], and Hamada-Johnston hard-core [17] interactions. The dependence of the deuteron polarization

components on the choice of the NN interaction has been studied in detail by Haftel et al. [10]. They calculated $T_{20}(\theta=0^{o})$ and $T_{21}(\theta=90^{o})$ in the range q=0 to 8 fm^{-1}. They employed many different models of the NN interaction differing in off-shell behavior and tensor force strength. They observed that the Reid soft core, Bonn, Paris, and Nijmegen potentials gave nearly equal results for both T_{20} and T_{21}. Only the Graz and Doleschall separable potentials gave different results.* (See ref.[10] for references to these NN interactions).

Thus they noted that the NN potentials with similar s-wave off-shell behavior give very similar results for T_{20} and T_{21} irrespective of their tensor force strengths, while those with different s-wave off-shell behavior result in measurably different T_{20} and T_{21}.** They have taken into account the pair-current contribution and the correction arising due to energy-dependence of the Bonn potential. However, their impulse approximation calculation is nonrelativistic, identical to the dashed curves in figs. 1 - 5. We have shown here and in refs. [6,7] that it is important to treat the relativistic kinematical effects in this problem carefully. Different assumptions regarding these effects lead to significantly different results for $A(q^2)$, $B(q^2)$, and the polarization components. For a quick comparison with the results of Haftel et al. [10] we plot in fig. 5 our results for $T_{20}(\theta=0^{o})$ and T_{21} $(\theta=90^{o})$ as a function of q fm^{-1}. It may be seen that the differences

*The Doleschall and Bonn potentials were unable to explain the $A(q^2)$ data when corrections to the impulse approximation were included [10]. Results for $B(q^2)$ were not presented in ref. [10].

**Similar suggestions were made by Moravcsik and Ghosh [9] and Hockert and Jackson [18].

between the various curves in fig. 5 are in fact larger than the differences that Haftel et al. found between the curves based on Reid soft-core, Bonn, Paris, and Nijmegen potentials, and are a sizable fraction of the differences that they found between the curves based on NN potentials differing in s-wave off-shell behavior. Hence due caution should be exercised while comparing calculated polarization transfers with the possible future measurements.

Very recently Allen and Fiedeldey[19] have also discussed the possibility of the polarization measurements being able to discriminate between the various deuteron wave functions. Their impulse approximation calculation is nonrelativistic, and they have not considered any meson-exchange current contribution. They calculated $T_{2\pm1}$ at $q \lesssim 6$ fm^{-1} for a family of phase equivalent deuteron wave functions with a percentage D state P_D varying from 4·5 to 7·5%. They concluded that measurements of $T_{2\pm1}$ at $q \lesssim 6$ fm^{-1} would not allow us to discriminate between all physically reasonable deuteron wave functions with different P_D.

In this paper our emphasis has been on comparing the predictions of the various theoretical approaches [4,7], rather than on studying the sensitivity of the polarization transfer to the various NN potentials; it being clear from the work of Haftel et al.[10] that T_{20} and T_{21} calculated with Reid soft core, Bonn, Paris, and Nijmegen potentials are nearly equal at $q \lesssim 6$ fm^{-1}. We conclude that measurements of polarization transfer in ed elastic scattering at high q^2 would be an important test of the various theoretical approaches trying to understand the structure of deuteron.

Acknowledgement

The author thanks Prof. S. A. Gurvitz and Prof. A. S. Rinat for a critical reading of the manuscript.

References

1. M. Gourdin, Phys. Rep. 11C (1974) 30.

2. R. G. Arnold, B. T. Chertok, E. B. Dally, A. Grigorian, C. L. Jordan, W. P. Schütz, R. Zdarko, F. Martin, and B. A. Mecking, Phys. Rev. Lett. 35 (1975) 776; and references therein. R. G. Arnold, B. T. Chertok, B. A. Mecking, S. E. Rock, I. A. Schmidt, Z. M. Szalata, R. C. York, and R. Zdarko, contributed paper at the 9th Int. Conf. on High Energy Phys. and Nucl. Structure, Versailles, France, (July 1981), p. 94.

3. F. Martin, R. G. Arnold, B. T. Chertok, E. B. Dally, A. Grigorian, C. L. Jordan, W. P. Schütz, R. Zdarko, and B. A. Mecking, Phys. Rev. Lett. 38 (1977) 1320; and references therein.

4. R. G. Arnold, C. E. Carlson, and F. Gross, Phys. Rev. C21 (1980) 1426.

5. see e.g.,M. Gari and H. Hyuga, Nucl. Phys. A264 (1976) 409.

6. R. S. Bhalerao and S. A. Gurvitz, Weizmann Inst. of Science preprint, submitted to Phys. Rev. Lett.; Weizmann Inst. of Science preprint, WIS-81/32/Jun-ph, Phys. Rev. C (in press).

7. S. A. Gurvitz, Weizmann Inst. of Science preprint, WIS-81/47/Oct-ph, submitted to Phys. Rev. D.

8. J. Scofield, Phys. Rev. 113 (1959) 1599, and ibid 141 (1966) 1352.

9. D. Schildknecht, Phys. Lett. 10 (1964) 254; M. Gourdin and C.A. Piketty, Nuovo Cim. 32 (1964) 1137; M. J. Moravcsik and J. Ghosh, Phys. Rev. Lett. 32 (1974) 321.

10. M. I. Haftel, L. Mathelitsch, and H. F. K. Zingl, Phys. Rev. C22 (1980) 1285.

11. R. G. Arnold, C. E. Carlson, and F. Gross, Phys. Rev. C23 (1981) 363.

12. R. Reid, Ann. Phys. (N.Y.) 50 (1968) 411.

13. see e.g., S. A. Gurvitz, Phys. Rev. C22 (1980) 725.

14. R. G. Arnold, private communication.

15. F. Iachello, A.D. Jackson, and A. Landé, Phys. Lett. 43B (1973) 191.

16. M. Lacombe, B. Loiseau, R. Vinh Mau, J. Côté, P. Pirès, and R. de Tourreil, Phys. Lett. 101B (1981) 139.

17. T. Hamada and I. D. Johnston, Nucl. Phys. 34 (1962) 382.

18. J. Hockert and A. D. Jackson, Phys. Lett. 58B (1975) 387.

19. L. J. Allen and H. Fiedeldey, Phys. Rev. C24 (1981) 1734.

Figure Captions.

Fig. 1a. Deuteron charge form factor $G_C(q^2)$. Reid soft-core NN interaction, and empirical dipole N form factors are used here and in all other figures. Dashed curve: non relativistic calculation, dotted curve: relativistic calculation with spectator N on-mass-shell, solid curve: relativistic calculation starting with the Bethe-Salpeter equation. The same convention is used in all other figures.

Fig. 1b. Deuteron quadrupole form factor $G_Q(q^2)$.

Fig. 1c. Deuteron magnetic form factor $G_M(q^2)$.

Fig. 2a. Deuteron form factor $S_S(q/2)$, see eq. (6).

Fig. 2b. Deuteron form factor $S_Q(q/2)$, see eq. (6).

Fig. 2c. Deuteron form factor $S_M(q/2)$, see eq. (6).

Fig. 3a. Polarizations p_x and $(p_{xx}-p_{yy})$ of the recoil deuteron in ed elastic scattering vs. the electron laboratory scattering angle θ. Longitudinally polarized electron beam (polarization=1) is incident on an unpolarized deuteron target. Curves are labelled by q^2 in $(GeV/c)^2$.

Fig. 3b. Same as fig. 3a for p_z and p_{xz}.

Fig. 3c. Same as fig. 3a for p_{zz}.

Fig. 4a-f. Polarizations p_x, p_z, p_{xz}, p_{zz}, $(p_{xx}-p_{yy})$, and p_x/p_{xz} of the recoil deuteron in ed elastic scattering for a fixed electron laboratory scattering angle $\theta=40^o$ vs. q^2. Longitudinally polarized electron beam (polarization=1) is incident on an unpolarized deuteron target.

Fig. 5. Polarizations $T_{20}(\theta=0^o)$ and $T_{21}(\theta=90^o)$ of the recoil deuteron in ed elastic scattering vs. q. Details as in fig. 4.

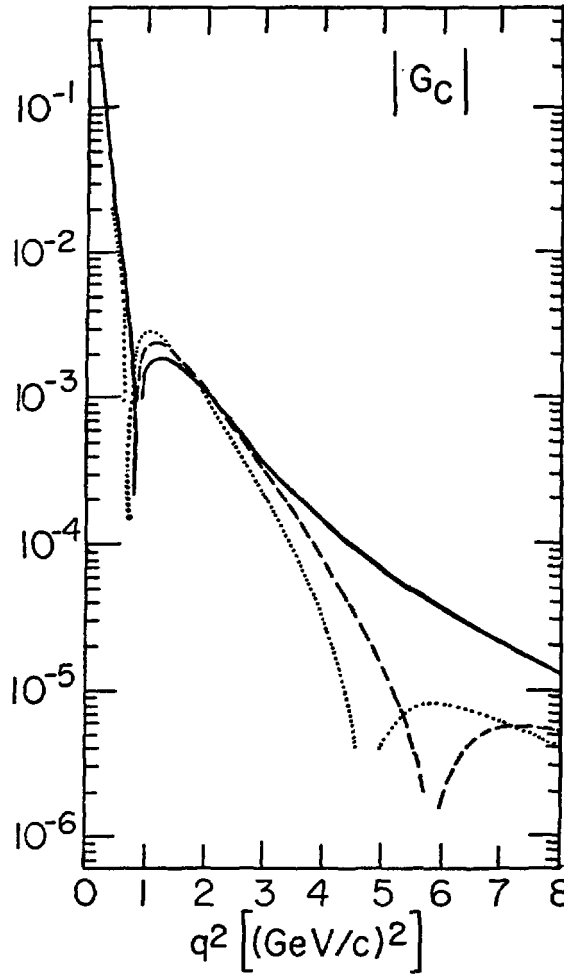

Fig. 1a

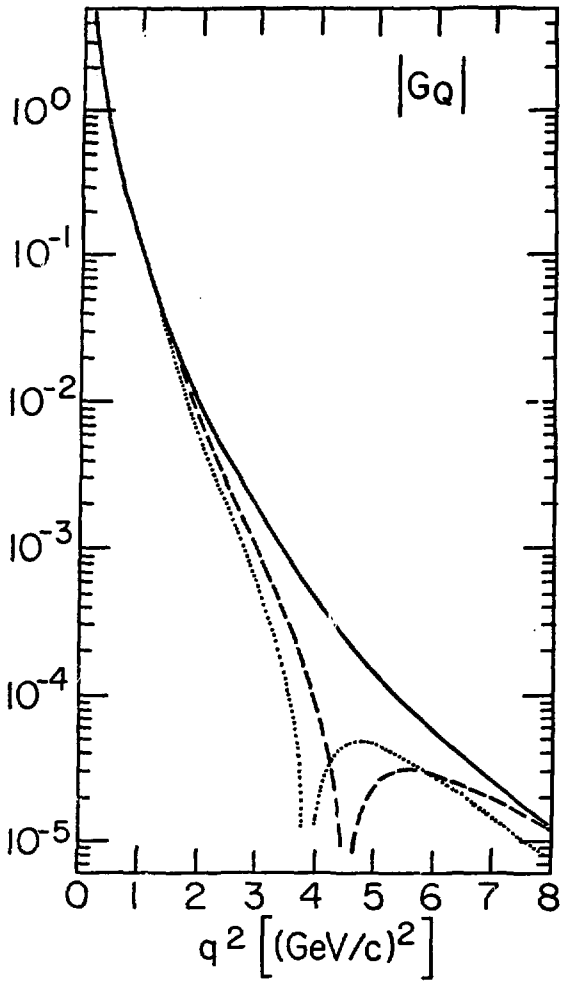

Fig. 1b

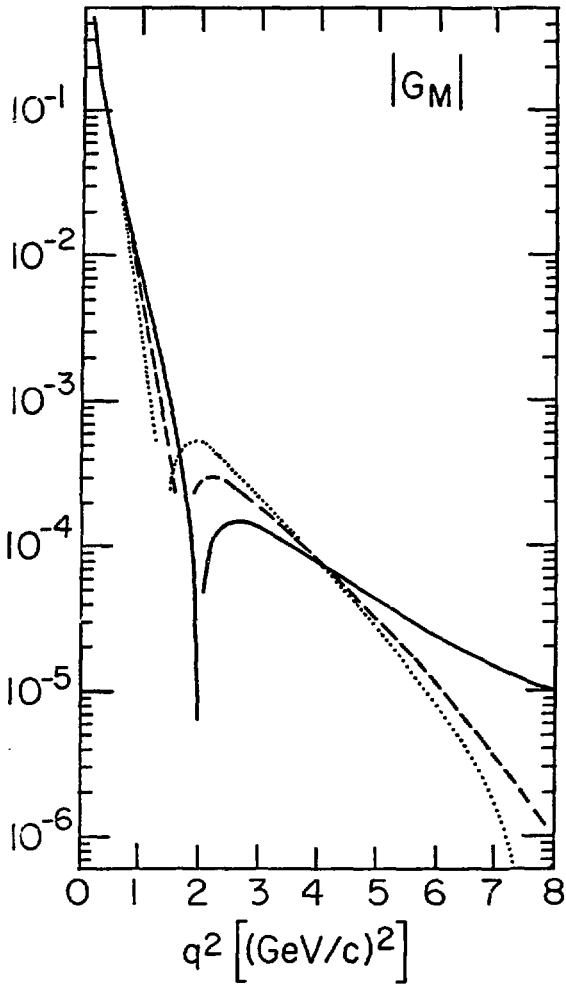

Fig. 1c

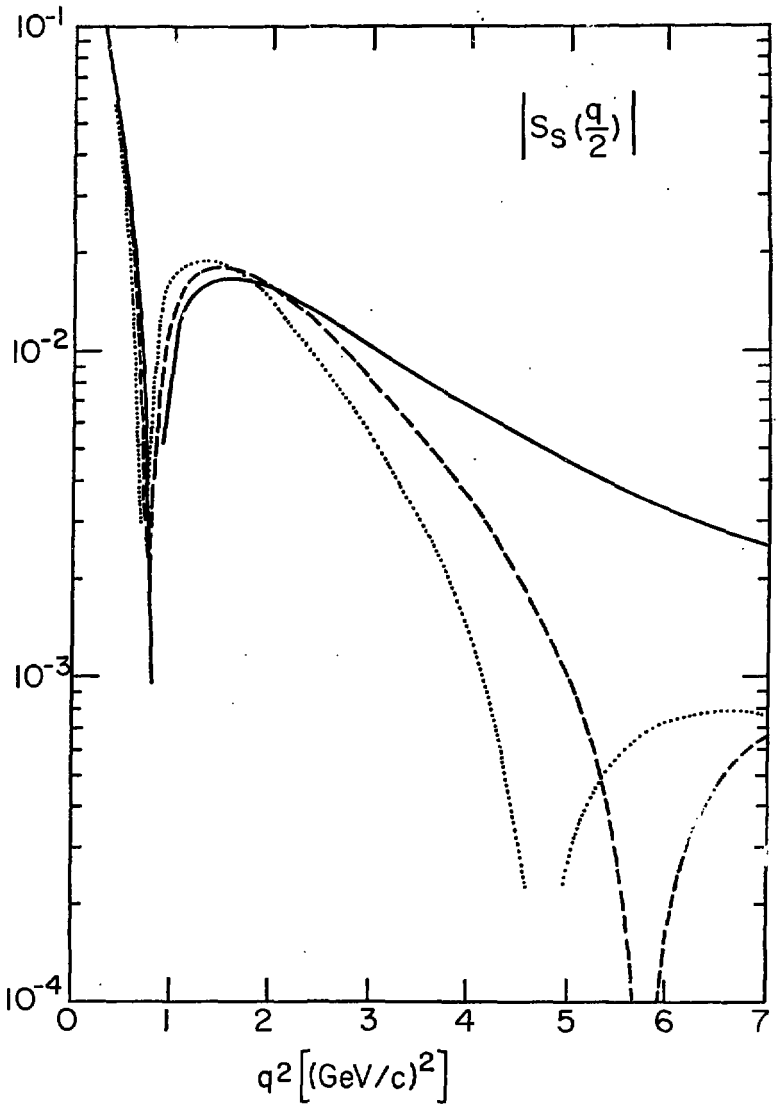
10^{-1}
10^{-2}
10^{-3}
10^{-4}
$\left|S_S\left(\frac{q}{2}\right)\right|$
0
1
2
3
4
5
6
7
$q^2\left[(GeV/c)^2\right]$

Fig. 2a

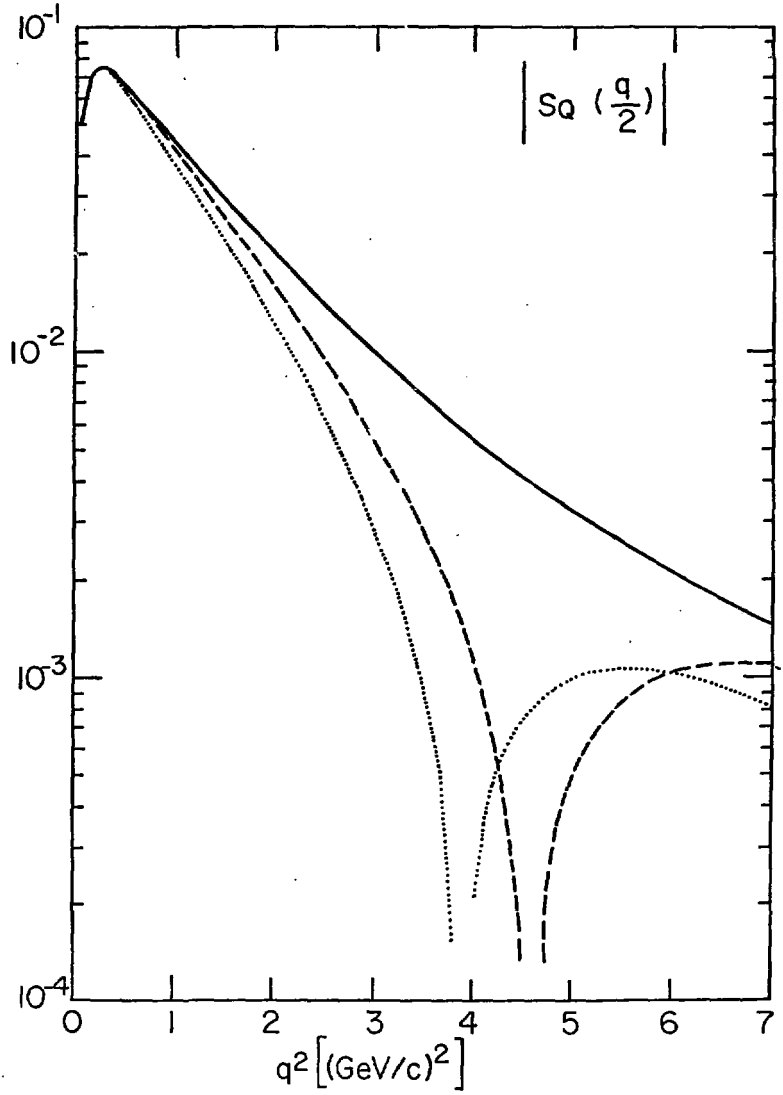
10^{-1}
10^{-2}
10^{-3}
10^{-4}
$\left|S_Q\left(\frac{q}{2}\right)\right|$
0
1
2
3
4
5
6
7
$q^2\left[(GeV/c)^2\right]$

Fig. 2b

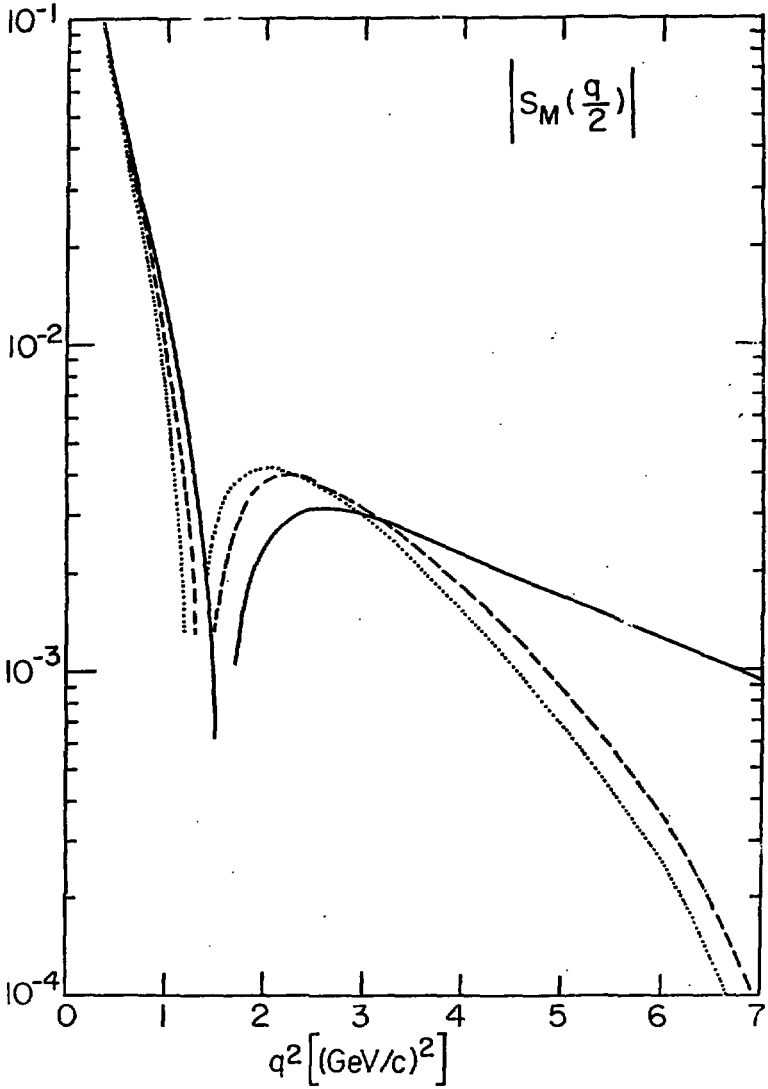
10^{-1}
10^{-2}
10^{-3}
10^{-4}
$\left|S_M\left(\frac{q}{2}\right)\right|$
0
1
2
3
4
5
6
7
$q^2\left[(\mathrm{GeV}/c)^2\right]$

Fig. 2c

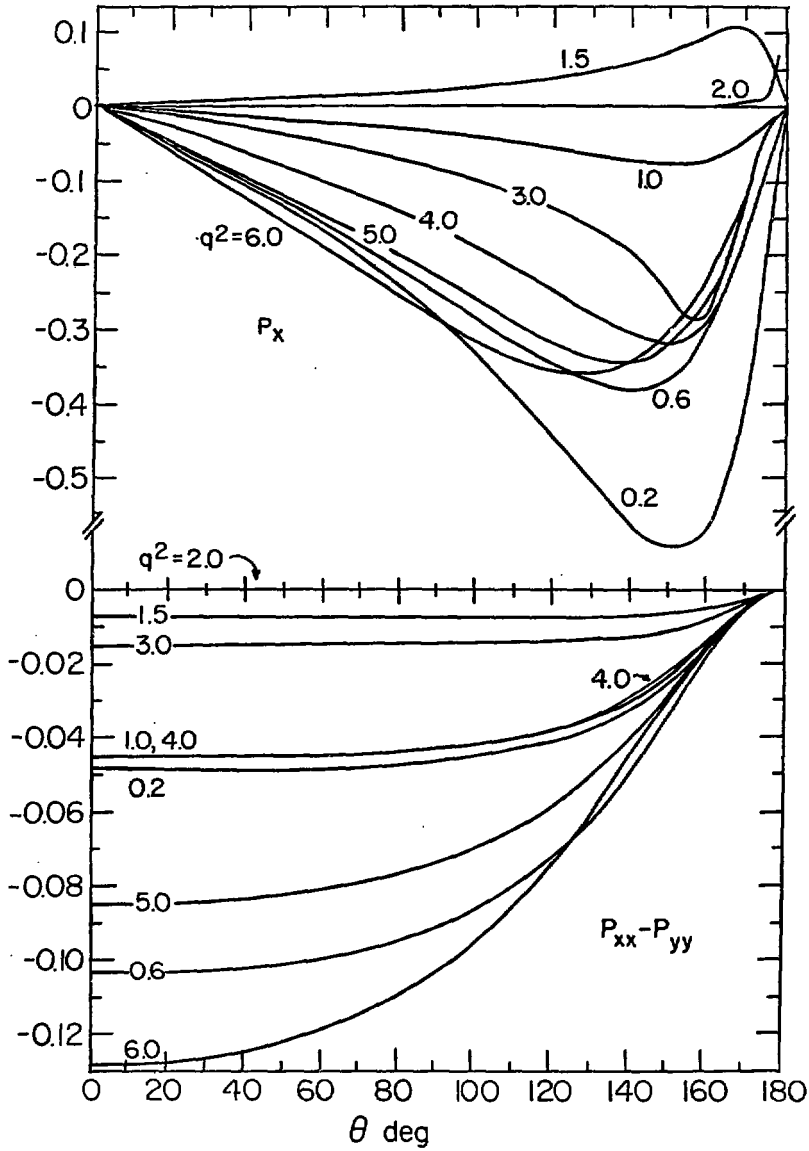
0.1
0
-0.1
-0.2
-0.3
-0.4
-0.5
1.5
2.0
1.0
3.0
4.0
5.0
q^2=6.0
P_x
0.6
0.2
q^2=2.0
0
-0.02
-0.04
-0.06
-0.08
-0.10
-0.12
1.5
3.0
4.0
1.0, 4.0
0.2
5.0
0.6
6.0
$P_{xx}-P_{yy}$
0
20
40
60
80
100
120
140
160
180
θ deg

Fig. 3a

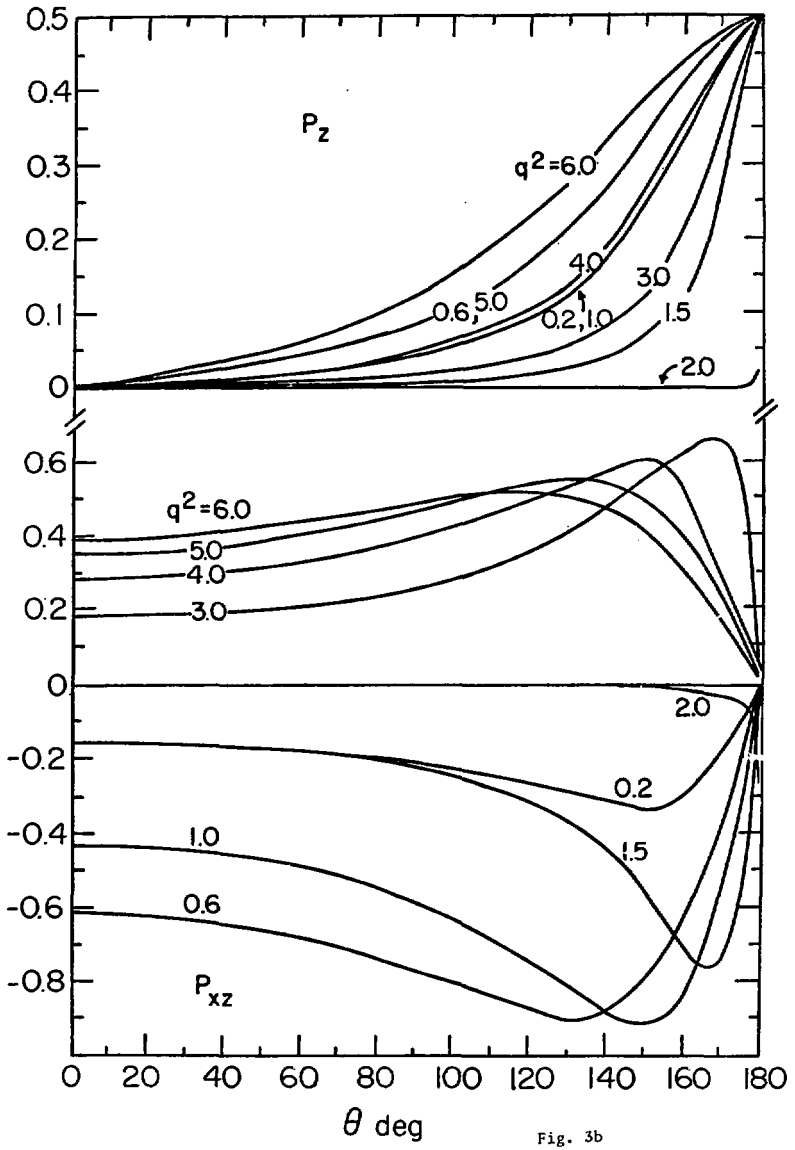
0.5
0.4
0.3
0.2
0.1
0
P_z
q^2=6.0
4.0
3.0
0.6,5.0
0.2,1.0
1.5
2.0
0.6
0.4
0.2
0
-0.2
-0.4
-0.6
-0.8
q^2=6.0
5.0
4.0
3.0
2.0
0.2
1.5
1.0
0.6
P_{xz}
0
20
40
60
80
100
120
140
160
180
θ deg

Fig. 3b

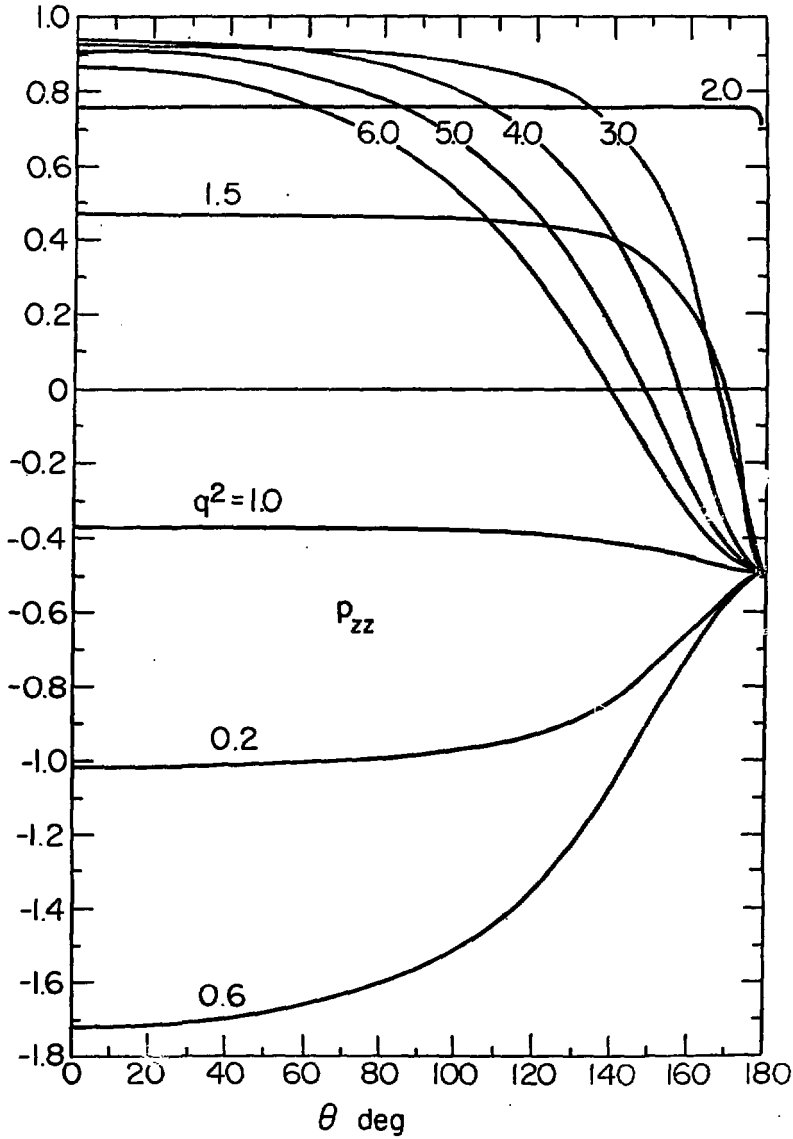
1.0
0.8
0.6
0.4
0.2
0
-0.2
-0.4
-0.6
-0.8
-1.0
-1.2
-1.4
-1.6
-1.8
0
20
40
60
80
100
120
140
160
180
θ deg
2.0
3.0
4.0
5.0
6.0
1.5
q² = 1.0
P_zz
0.2
0.6

Fig. 3c

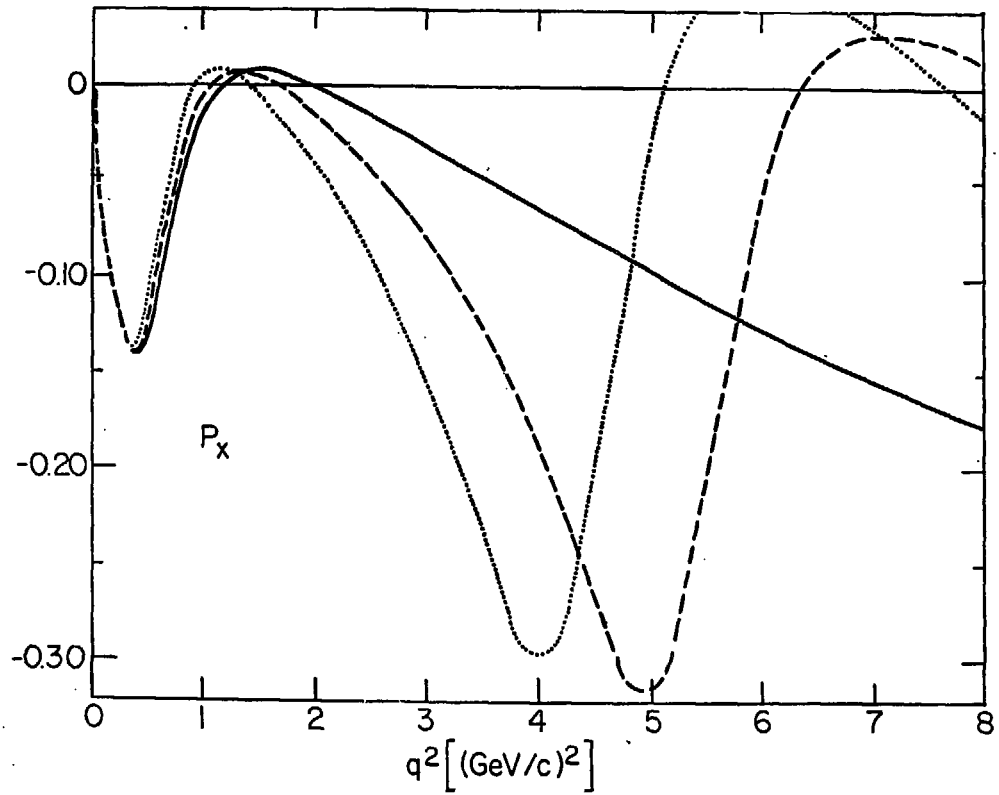

Fig. 4a

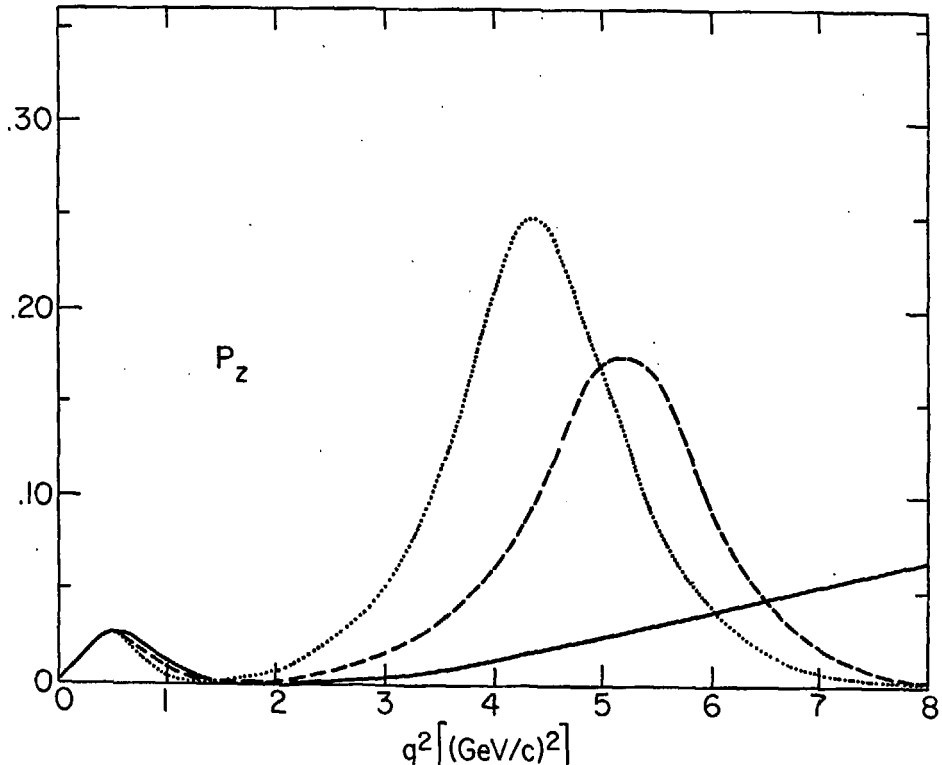

Fig. 4b

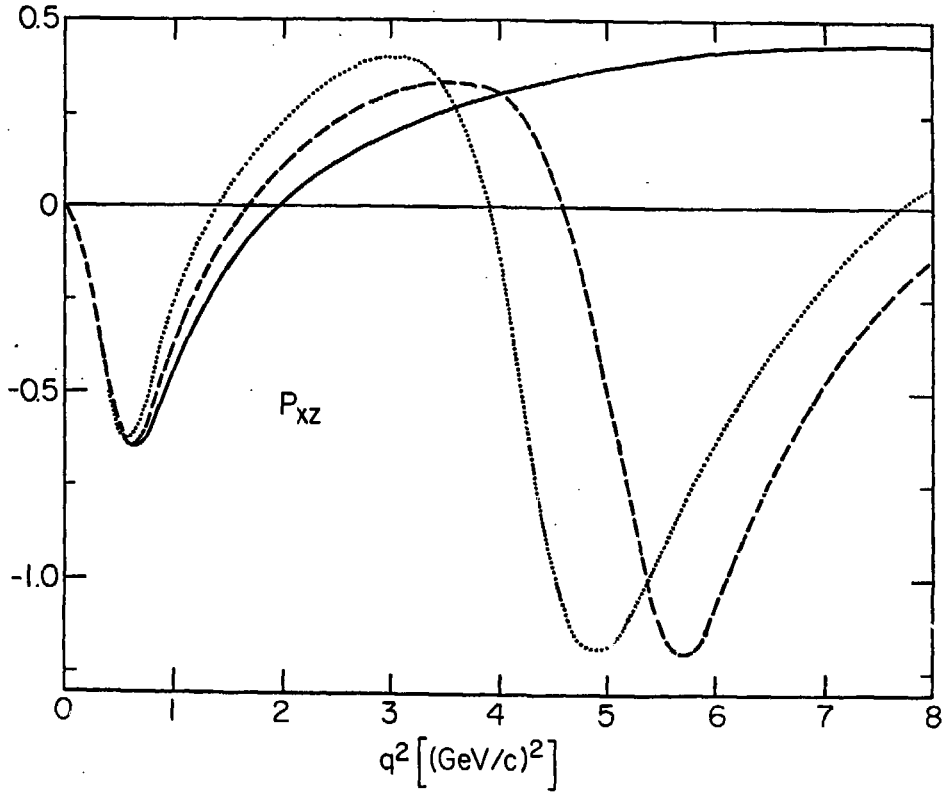

Fig. 4c

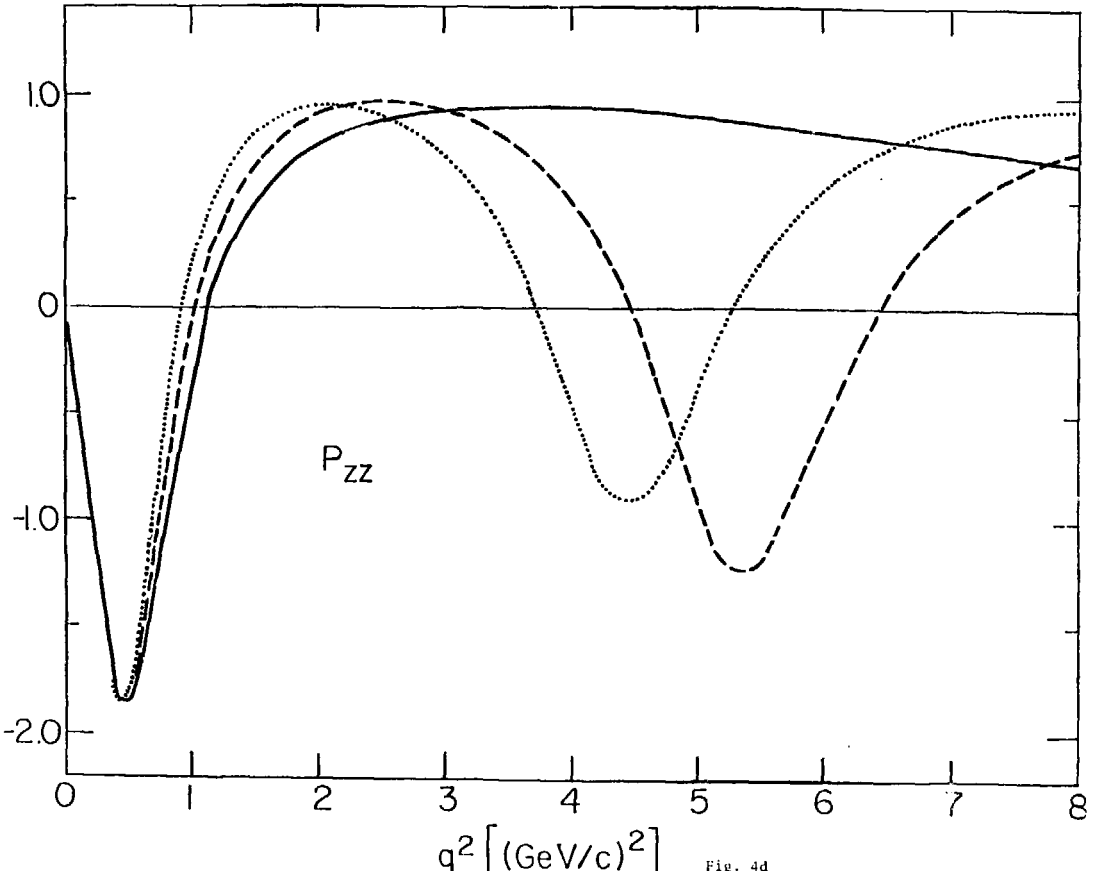

Fig. 4d

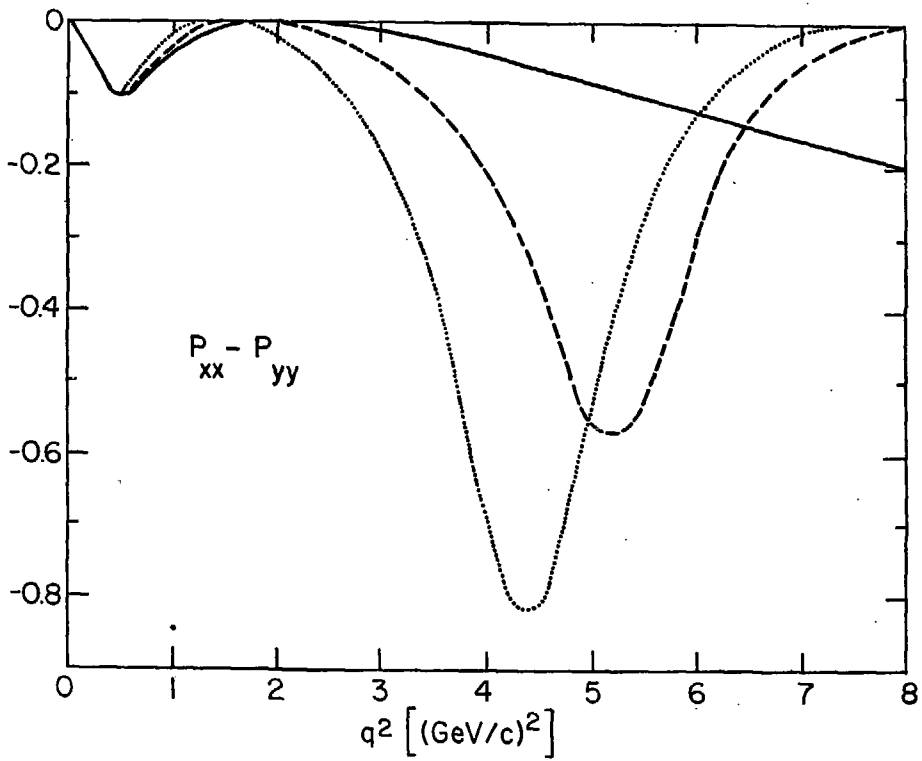

Fig. 4e

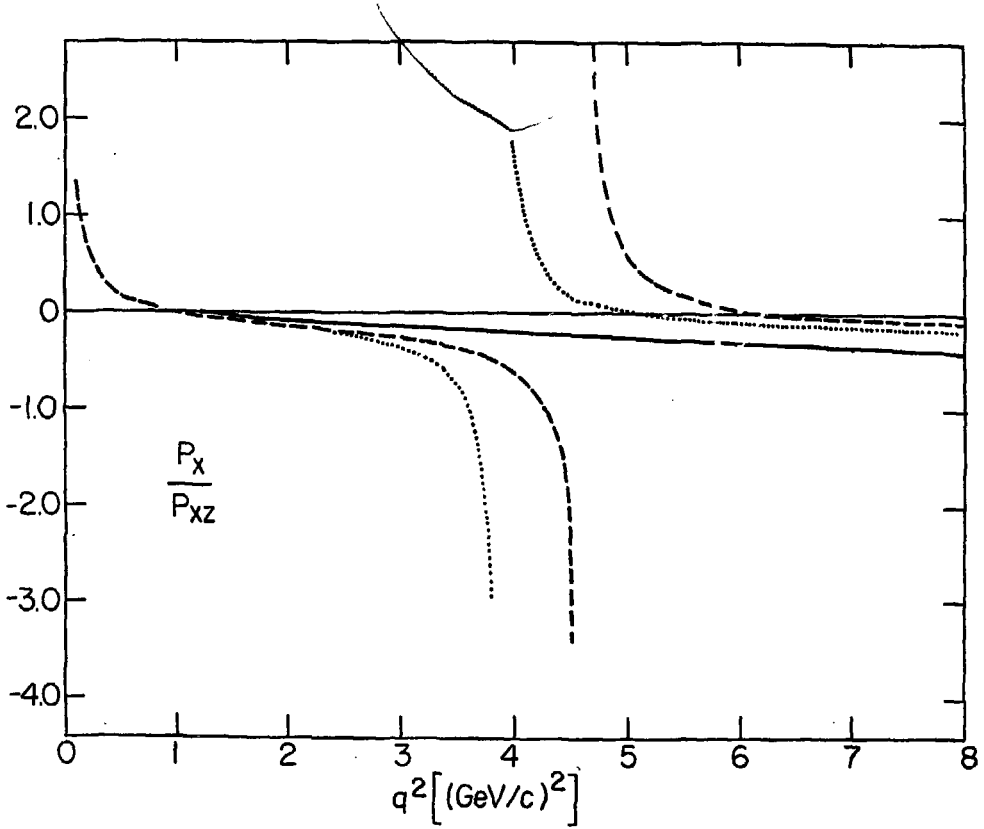

Fig. 4f

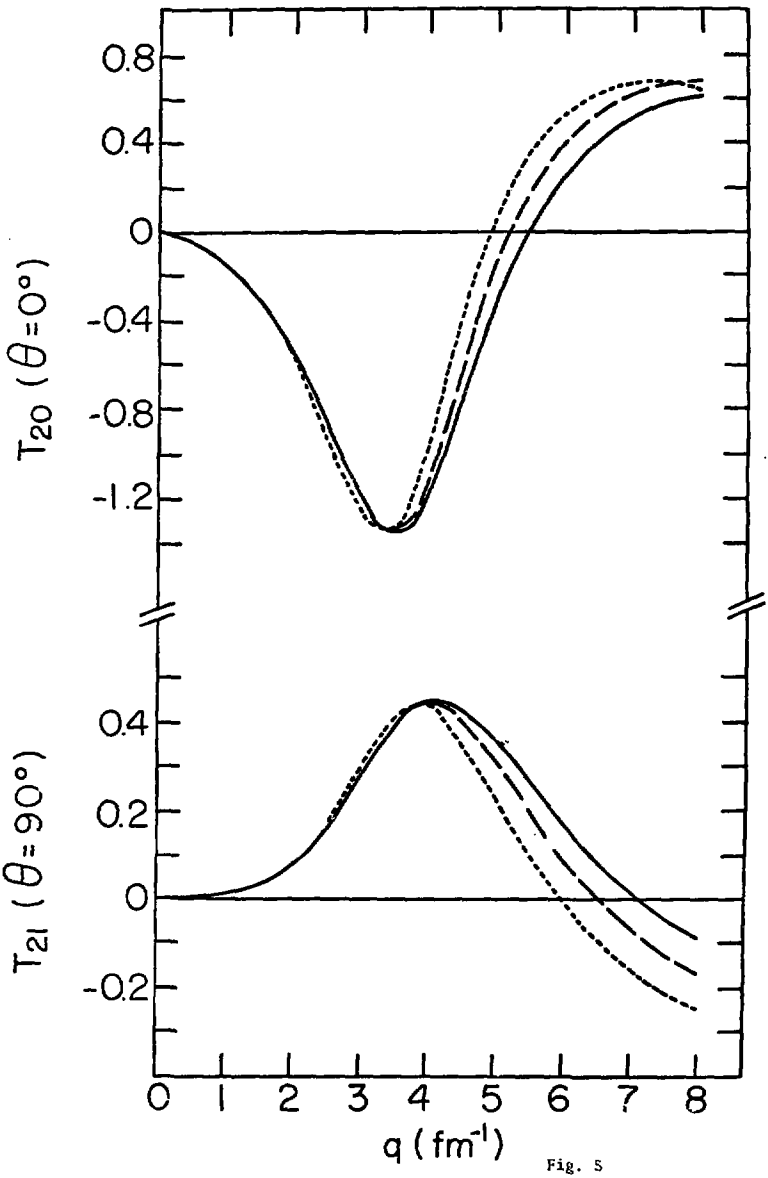
0.8
0.4
0
-0.4
-0.8
-1.2
T_{20} (θ=0°)
0.4
0.2
0
-0.2
T_{21} (θ=90°)
0 1 2 3 4 5 6 7 8
q (fm^{-1})

Fig. 5